ISBN: 978-3-95450-132-8 doi:10.18429/JACoW-IPAC2014-WEPRI053

PHASE METHOD OF MEASURING CAVITY QUALITY FACTOR

O. Melnychuk*, R. Pilipenko, A. Pischalnikov, W. Schappert, D.A. Sergatskov
Fermi National Accelerator Laboratory, Batavia, IL 60510, USA

Abstract

Novel method for measuring intrinsic quality factor of superconducting RF (SRF) cavities using both amplitude and phase information of forward, reflected, and transmitted cavity signal is discussed. Advantages of the method in comparison with traditional types of cavity quality factor measurements are highlighted. Computer simulations and evaluation of uncertainties for the measurements are described. Analysis of data collected at vertical test facility for SRF cavities at Fermilab is presented.

INTRODUCTION

Characterization of superconducting radio-frequency (SRF) cavity involves measuring intrinsic quality factor Q_0 as a function of accelerating field E_{acc} in a vertical test stand (VTS) [1]. Q_0 can be expressed as

$$Q_0 = Q_L(1+\beta_1) \tag{1}$$

where Q_L is a loaded quality factor and β_1 is a coupling parameter defined as $\beta_1 = Q_0/Q_1$, where Q_1 is RF input port quality factor. Field probe quality factor is assumed to be infinite. Uncertainty on Q_0 is controlled by the β_1 uncertainty. The focus of this paper is accurate measurement of β_1. Standard measurement technique [2] relies on power measurements of forward and reflected RF signals, in which phase information is averaged out. Reduction of information through averaging naturally leads to increase of the uncertainty of Q_0 measurement. Q_0 uncertainty is estimated to be approximately 4% and 25% for β_1 between 0.5 and 2.5 and β_1=10 respectively [3]. Additional uncertainty due to cross-contamination of forward and reflected signal, which was not included in these estimates is expected. Technique described in this paper allows to measure Q_0 with a significantly improved accuracy in a much wider range of β_1. Improvement in accuracy is attributed to using full rather than averaged information in the data and compensating for signal cross-contamination in the data analysis.

METHOD

Cavity transfer function $T_{P/F}$ is defined as the ratio of the cavity voltage and the forward signal voltage

$$T_{P/F} = \frac{V_{cavity}}{V_F} = \frac{2}{1+\beta^{-1}+i(1+\beta^{-1})X} \tag{2}$$

where $X = \frac{\omega_{RF}-\omega_{cav}}{\omega_{1/2}}$, ω_{RF} and ω_{cav} are RF drive frequency and cavity resonance respectively, $\omega_{1/2}$ is related to cavity decay time τ_L as $\tau_L = (1/2)\times\omega_{1/2}$. Subscripts 'P' and 'F' denote cavity (probe) and forward signal respectively. $T_{P/F}$ is equivalent to S_{21} scattering parameter defined in Equation (11) with indices '2' and '1' corresponding to transmitted (output, cavity) and forward signal respectively. Similarly transfer function $T_{P/R}$ can be defined as the ratio of the cavity voltage and the reflected signal voltage. Because of boundary conditions $V_{cavity} = V_F + V_R$ [4], cavity transfer functions satisfy $T_{P/F} + T_{P/R} = 1$ constraint. $T_{P/F}$ and $T_{P/R}$ appear as ellipses in the complex plane as ω_{RF} is swept across the cavity resonance.

For the purposes of data analysis, it is more convenient to work in terms of inverse transfer functions $T^{-1}_{P/F}$ and $T^{-1}_{P/R}$ that are given by equations (3) and (4) respectively

$$T^{-1}_{P/F} = \frac{1}{2}\times[1+\beta^{-1}+i(1+\beta^{-1})X] \tag{3}$$

$$T^{-1}_{R/F} = \frac{1}{2}\times[1-\beta^{-1}-i(1+\beta^{-1})X] \tag{4}$$

Inverse transfer functions appear as straight lines in the complex plane. Inverse transfer functions also satisfy $T^{-1}_{P/F} + T^{-1}_{P/R} = 1$ due to the same boundary conditions that were mentioned above. Coupling parameter β_1 can be extracted from the sum of the the two functions as

$$\beta_1^{Measured} = \frac{1}{Re\{< T^{-1}_{P/F} - T^{-1}_{P/R} >\}} \tag{5}$$

In Equation (5) symbols '<>' indicate averaging over the sample of data points that are taken at different values of ω_{RF}. In practice, it was the phase difference between the probe and forward signal that was changing while ω_{RF} value was kept fixed.

Equation (5) was derived under the assumption of perfect calibration of probe, forward and reflected signal. In practice, each signal is associated with an a priori unknown complex gain, G, which depends on the specifics of the hardware. Only two relative gains for 'P' signal with respect to 'F' and 'R' are of interest rather than three absolute gains since we work with the transfer functions. In the presence of relative gains the RHS of equations (3) and (4) need to be multiplied by respective complex gain factors. Consequently equation (5) will no longer hold. However, complex gains can be calibrated out by dividing the gain multiplied transfer functions by their corresponding derivatives with respect to $X' = (1+\beta^{-1})X$ according to:

$$T^{-1} = \pm i(T^{-1}\times G)/\frac{d(T^{-1}\times G)}{dX'} \tag{6}$$

where additional factor of $\pm i$ corresponds to $T^{-1}_{R/F}$ and $T^{-1}_{P/F}$ function respectively.

* alexmelnitchouk@gmail.com

ISBN: 978-3-95450-132-8 doi:10.18429/JACoW-IPAC2014-WEPRI053

In the data analysis where β_1 is not known, in the presence of complex gains $\beta_1^{Measured}$ can be obtained as follows. First inverse transfer functions need to be divided by their differentials (averaged variation of the transfer function between adjacent frequency sweep points) Thus modified transfer functions are corrected for phase and gain differences. In the final step absolute calibration is performed by making use of $T_{P/F}^{-1} + T_{P/R}^{-1} = 1$ constraint. Each transfer function is divided by the averaged sum of their real parts. In the end coupling parameter β_1 is determined according to Equation (7)

$$\beta_1^{Measured} = \frac{Re\{< T_{P/F}^{-1} + T_{P/R}^{-1} >\}}{Re\{< T_{P/F}^{-1} - T_{P/R}^{-1} >\}} \qquad (7)$$

Figures 1 and 2 show simulated $T_{R/F}^{-1}$ and $T_{P/F}^{-1}$ transfer functions as well as their sum without and with the effects of finite directivity, complex gains,and noise in the simulation respectively. Frequency was spanned in the range of approximately [-7f_{12}, +7f_{12}] around the center frequency and O(1000) samples were used. Cross-contamination of

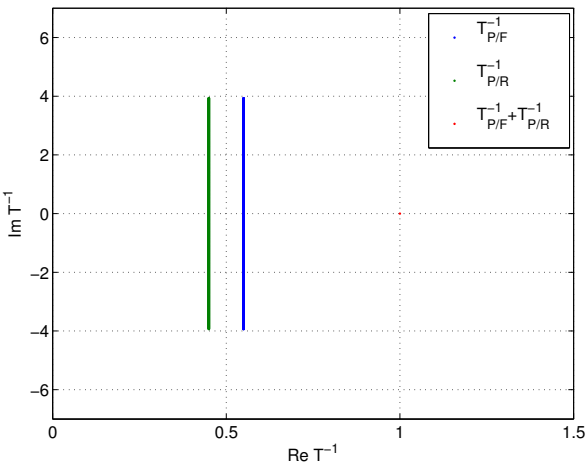

Figure 1: Inverse transfer functions $T_{P/F}^{-1}$, $T_{P/R}^{-1}$ in the ideal case. Separation between the two vertical lines along the horizontal axis is equal to β_1^{-1}. Length of the two vertical lines along the vertical axis depends on the range of RF drive frequency span across the resonance relative to f_{12} of the cavity.

forward and reflected signal leads to a perturbation of the inverse transfer function. The amount and the direction of the perturbation in the complex plane is controlled by the directivity of the directional coupler (the smaller the directivity, the larger the contamination, the larger the perturbation) and the phase difference between the forward and reflected signal. Variation of the phase difference over the full cycle, at a fixed detuning, corresponds to a circle in the complex plane centered at the point of the non-contaminated case. Radius of the circle increases with the amount of contamination (decreases with the increase of directivity). By sweeping the phase difference over the cycle with the dedicated hardware setup and finding the center of the corresponding circle,

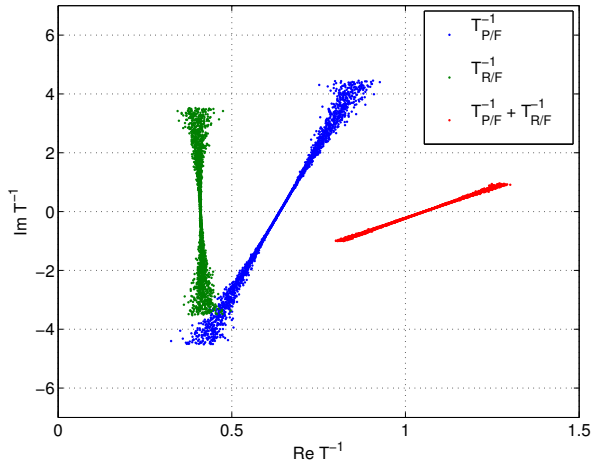

Figure 2: Inverse transfer functions $T_{P/F}^{-1}$, $T_{P/R}^{-1}$ and their sum with the simulation of finite directivity, relative complex gains and typical noise.

the effect of finite directivity on measured β_1 accuracy is reduced by orders of magnitude.

DATA

The experimental configuration is shown schematically in Figure 3. The cavity was driven by a 1W amplifier con-

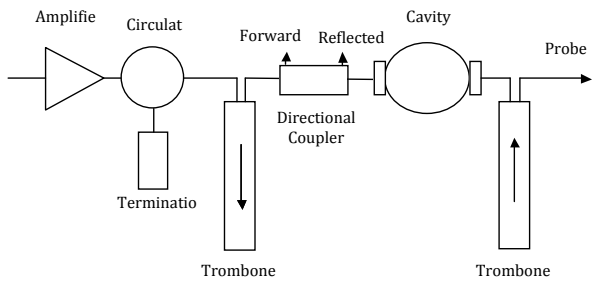

Figure 3: Experimental configuration.

trolled by the VTS analog CW tracking LLRF system. Phase-locked-loop (PLL) was used in the probe circuit for locking the signal to the cavity resonance.The cavity incident and reflected RF signals were monitored using a Hewlett Packard HP776D directional coupler (20 dB coupling, 40 dB directivity) inserted into cavity power circuit. RF signals were down-converted to 13 MHz intermediate frequency (IF) using an eight channel transceiver provided by the Fermilab AD/LLRF group. IF signals from the transceiver were captured using a Lyrtech VTS-16ADC processing board with 8 channels of 14-bit ADCs running at a clock speed of 104 MHz. The IF signals were converted to baseband by firmware in the Xilinx IV SX55 FPGA and recorded to memory onboard the Lyrtech. The recorded baseband data was read from the Lyrtech by a MATLAB program running on PC and stored to disk. General Radio 874-LTL trombone was inserted in the drive circuit and a second trombone was inserted in the probe circuit. Each trombone was mounted on a Zaber T-LSR 150 B motorized stage to

ISBN: 978-3-95450-132-8 doi:10.18429/JACoW-IPAC2014-WEPRI053

allow the length of the drive cable and the phase between the forward and probe signals to be varied independently. As the baseband data were being recorded, the length of the each of the two trombones were synchronously swept together over one wavelength in such a way as to keep the relative phase between the forward and probe signals constant while the length of the cable varied. Data were recorded for 12 trombone positions. For each trombone position phase sweep across the cavity resonance was performed by offsetting probe signal phase incrementally with the total of O(10) points in the sweep. With these data β_1 was measured with

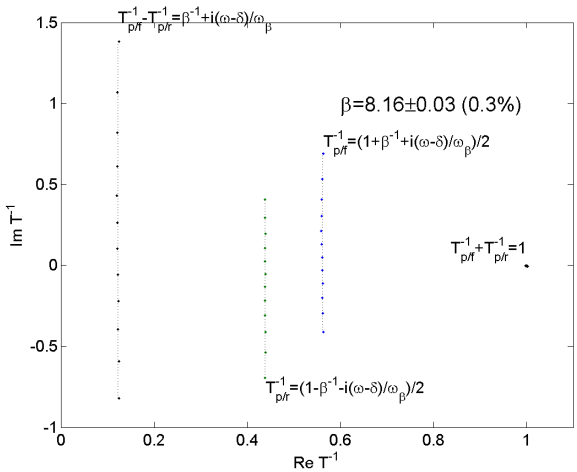

Figure 4: Measurement of β_1 in VTS data

statistical precision of 0.3%.

SIMULATION

Simulation of RF cavity operation in terms of complex incident, reflected and transmitted RF signals is performed with MATLAB program with Signal Processing Toolbox [5]. Simulation includes the following effects: i) finite directivity of directional coupler; ii) random gain and phase shift associated with a priori unknown attenuation and length of cables; ii) noise (complex Gaussian model). Cavity parameters were chosen according to typical performance of 1.3GHz TESLA-shaped elliptical cavity that underwent standard ILC recipe treatment (intrinsic quality factor $Q_0 = 2.0^{10}$) at VTS. Effect of finite directivity of the directional coupler on the measured forward and reflected signals was simulated according to

$$V_f^{Measured} = V_f^{TRUE} + \frac{V_r^{TRUE}}{10^{D/20}} \quad (8)$$

$$V_r^{Measured} = V_r^{TRUE} + \frac{V_f^{TRUE}}{10^{D/20}} \quad (9)$$

where subscripts 'f' and 'r' refer to forward and reflected signal respectively and D is the directivity of the directional coupler defined as

$$D = 10log(\frac{P_3}{P_4}) \equiv 20log(\frac{S_{31}}{S_{41}}) \equiv 20log(\frac{S_{31}}{S_{32}}) \quad (10)$$

where P_i is outgoing power level measured at coupling port i and S_{ij} are scattering parameters for ports i and $j$defined as

$$S_{ij} = \left.\frac{V_i^-}{V_j^+}\right|_{V_k^+=0 \text{ for } k\neq j} \quad (11)$$

where superscripts '+' and '-' correspond to incoming and outgoing signals respectively and the ports of the directional coupler are labelled as follows: 1 – input port, 2 – output port, 3 – coupling port that corresponds to input port, 4 – coupling port that corresponds to output port. Directivity and scattering parameter definitions according to [4] were used. Noise level was $O(10^{-6})$, which corresponds to typical $O(10^{-3})$ noise level after averaging the data over $O(10^{-6})$ samples.

SUMMARY

Q_0 measurement technique based on using complex signal information was described. Error on β_1 due to finite directivity as a function of phase difference between forward and reflected signal shown in Fig. 5 Maximum error on β_1

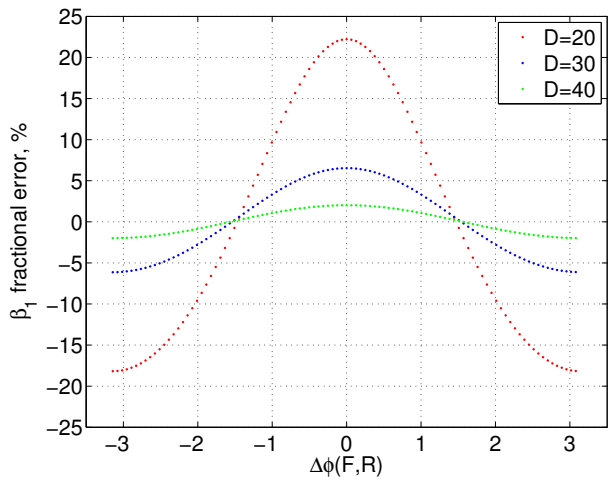

Figure 5: Fractional error on β_1 in MATLAB simulation as a function of phase difference between forward and reflected signal. Red, blue, and green correspond to directional coupler directivity of 20, 30, and 40 respectively. Simulation was performed for β_1=10.

due to finite directivity when forward and reflected signals are in phase is 22%, 7% and 2% for directivity of 20, 30 and 40 respectively. After signal cross-contamination effect due finite directivity is compensated for at the data analysis stage, fractional systematic error on β_1 is 6×10^{-4} for β_1=10. Fractional systematic error on β_1 is defined as fractional difference between measured and true value of β_1. Statistical precision of the measurement is 7×10^{-6} (standard deviation) in the simulation. In real data analysis statistical precision of the measurement is 3×10^{-3} (standard deviation).

ISBN: 978-3-95450-132-8 doi:10.18429/JACoW-IPAC2014-WEPRI053

REFERENCES

[1] Padamsee H., *RF Superconductivity for Accelerators*, second edition, (New York: Wiley, 2008)

[2] T. Powers, “Proceedings of he 12th Workshop on RF Superconductivity", SuP02 (2005)

[3] O. Melnychuk, “Proceedings of he 16th Workshop on RF Superconductivity", THP095 (2013)

[4] David M. Pozar, *Microwave Engineering*, 4-th edition, (Wiley-VCH, 2011)

[5] MATLAB Release 2013b with Signal Processing Toolbox 6.20, The MathWorks, Inc., Natick, Massachusetts, United States